IOSR Journal of Mechanical and Civil Engineering (IOSR-JMCE)
e-ISSN: 2278-1684,p-ISSN: 2320-334X, Volume 19, Issue 4 Ser. III (Jul. – Aug. 2022), PP 08-23
www.iosrjournals.org

3D Laser Scanningand Close-Range Photogrammetryfor Observation and Measuring the Reinforced Concrete (RC) StructuralCracks& Deflection

Magda Farhan, HossamEldinFawzy and Reham Kandeel
Department of Civil Engineering, Faculty of Engineering, Kafr El-Sheikh University, Kafr El-Sheikh,Egypt.

Abstract
The existence of cracks and deflections in a reinforced concrete structure is a matter of great importance and have been under study for many decades. In many cases, such cracks or deflections might represent a sign of danger to the structure. Hence, it is indeed important to accurately study and monitor the development of these cracks and deformations. In this study, two surveying techniques (Laser scanning and close range photogrammetry) have been used in addition to Linear Variable Differential Transformer (LVDT) to monitor the width of cracks in reinforced concrete beam. Also, laser scanning, close range photogrammetry and another surveying technique that is total station, in addition to Electronic Digital Vernier have been used to monitor the deflection of the reinforced concrete beam. The most obvious advantage of surveying techniques is that they don't require direct contact with the target under observation. The results obtained by all these methods are compared to provide a clearer view which proves that modern surveying techniques can provide accurate results in a fast way compared to traditional methods.
Keywords: *Cracks; Deflection; Total Station; Digital Close-Range Photogrammetry; Terrestrial Laser Scanner.*

Date of Submission: 07-08-2022 Date of Acceptance: 22-08-2022

I. Introduction

Reinforced concrete is one of the most widely used construction materials in the last 200 years. This is due to many advantages such as that it is low cost, easy to produce and easy to cast into different forms to give many complicated shapes. So, it is important to control and monitor the quality, durability and strength of reinforced concrete structures to ensure the structure will not lose its functionality and also will not lose the final look of the structure.For this reason, cracks areconsidered one of the most important factors that provide indications that the structure needs to be monitored as cracks not only causes bad looking of the structure, but also they indicate (in some cases) that the structure is no longer safe for human use. There exist many causes for cracks in a reinforced concrete element, but the fundamental reason is that whenever a concrete member is subjected to a tensile stress greater than the strengthof the member, cracks will occur. This is probably the major disadvantage of concrete, as it is known that concrete has very low tensile strength compared to the compressive strength of concrete.

In general, these causes can be briefly classified as structural and nonstructural cracks. Structural cracks are those induced in the reinforced concrete element when the applied load to the element exceeds the design limit. On the other hand, the most common causes of nonstructural cracks are (dry shrinkage, thermal shrinkage, plastic shrinkage and RC fragmentation andthe reinforcement steel barsoxidation) [1-3]. Also, the relation between the cracks and the oxidation of steel reinforcement is implicit. This is because when cracks exist, they form a path for water and other substances to penetrate the reinforced concrete member and eventually reach the steel reinforcement, thus causing oxidation of the steel bars, then steel bars expand due to corrosion which finally causes more cracks and the cycle keeps going on. It is proved that reinforcement steel bars oxidation increases by the increasing of cracks thickness over 1 mm [4].

Manytraditional methods have been used in the past years to obtain the necessary data of some target object as described before. In the case of detecting structural deformations, wire strain gauges, laser sensors, gypsum patches and LVDT are all common methods used to monitor cracks and deformations in a reinforced concrete element [5].

There exist many survey technologies that have a major function of getting the coordinates of any target under observation, such as: GPS, Total stations, remote sensing, photogrammetry, Laser scanning and others. Each of them has its own advantages and disadvantages considering cost, accuracy of measurement, distance covered and others. The following figure illustrates the relationship between target object size, accuracy and relevant technology [6].

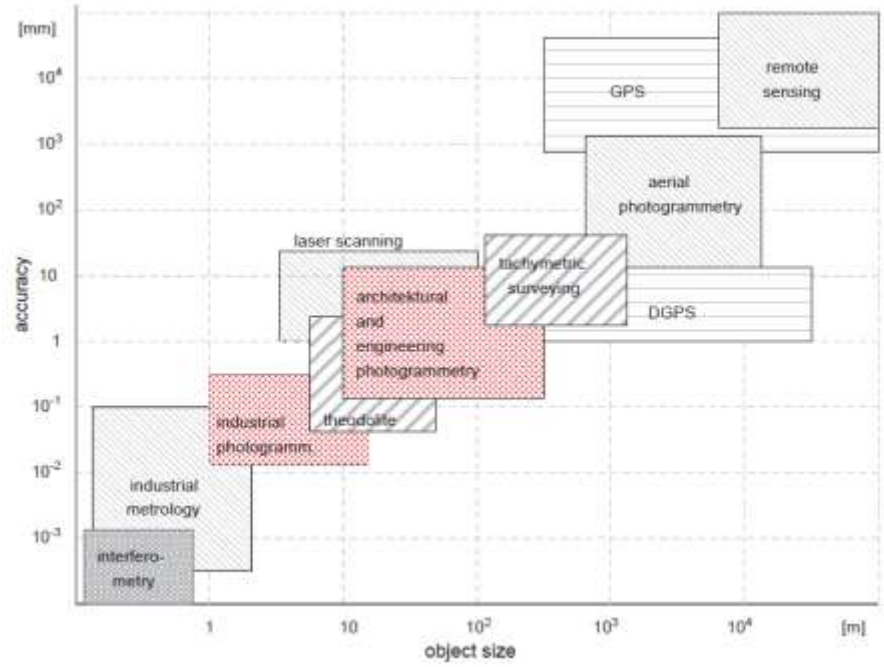

Figure 1: The relationship between target object size, accuracy and relevant technology

In this research, we will make use of only three surveying techniques: total station, Close Range Photogrammetry (CRP) & Terrestrial Laser Scanner (TLS).

Photogrammetry is a method of big interest for many engineeringfields and has been used since 1850s in many applications that were mainly focusing on documenting architectural structures and monuments [6]. It is also used in many modern studies along with laser scanners in civil engineering applications for measuring cracks and deformations in civil structures like bridges, dams, shells, etc. [7-18]. Also, both technologies are used in architectural engineering to generate 3D models and obtain different dimensions of timber structures, trusses and facades[19], [20]. Photogrammetry is also used in archaeology to produce documentationand 3D models of historical buildings [21], [22]. Photogrammetry also found its way in industrial applications as it is used as a very useful solution in different problems that made use of the greatest advantage of the technology which is that it doesn't require close contact with the target object[23], [24].

Finally, one of the greatest outcomes of thesetechniques (Photogrammetry &laser scanners) is the possibility to obtain a large amount of very dense points called "point cloud" which can be used to generate very sophisticated 3D models which is are used to do further engineering analysis and studies.[25], [26], [27].

The goal of this study is to use surveying techniques (Photogrammetry & laser scanners) to detect and monitor thecracks and deflection in a reinforced concretestructure.The 3D measurements obtained by these techniques and those obtained by traditional methods are compared together to provide a better view on the accuracy and error of the proposed surveying techniques.The experiment was done on a reinforced concrete beam prepared in the material lab at the University of Kafr El-sheikh, then the beam was loaded and tested by a 4-point load test. Photo-modeler and Topcon Scan Master software were used to extract 3D data of the measured beam deflection and measured cracks.

II. Methodology

In this paper, we will use four techniques and will compare their results, which are:

- Linear Variable Differential Transformer (LVDT) which is used to measure the deflection of the beam and Electronic Digital Vernier which is used to measure the crack width.
- Total station: used to measure the deflection of the loaded beam.
- Photogrammetry: used to create 3D model of the observed beam and obtain 3D measurements of the beam deflection and also cracks width.
- Laser scanners: used for the same purpose like photogrammetry as an alternative that provides dense amount of scanned points under the name of "point cloud" that is used to create 3D models of the observed beam and obtain 3D measurements for cracks and deflection.

II.I LVDT

A LVDT is an electromechanical passive (not capable of generating energy) inductive position transducer that can convert linear motion (better to say, rectilinear motion), when mechanically coupled to the target object, into a corresponding electrical signal as shown in the following figure (2).

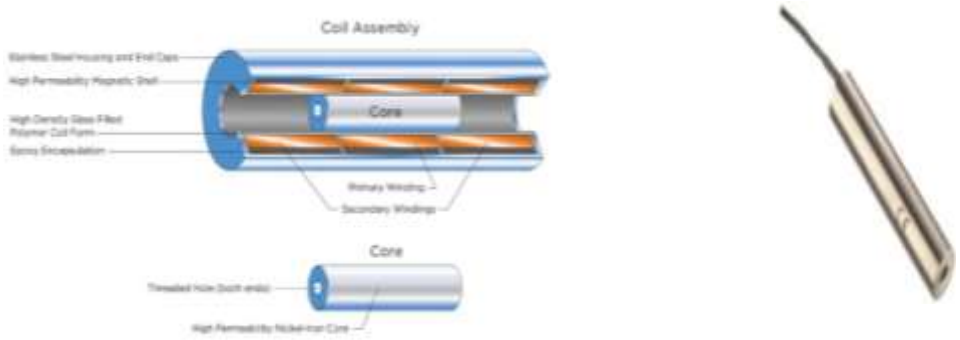

Figure 2: LVDT device

II.II Digital Vernier

The digital Vernier (or calipers) is a precision instrument useful in taking accurate linear measurements like depth, diameters, lengths, etc. It is available in many sizes (150 mm, 300 mm and up to 2000 mm) and vary in the accuracy and resolution depending on the manufacturer and some Vernier devices can reach resolution of 0.01 mm. It also available with digital display to obtain the reading of the caliper instead of manually reading the measurement.

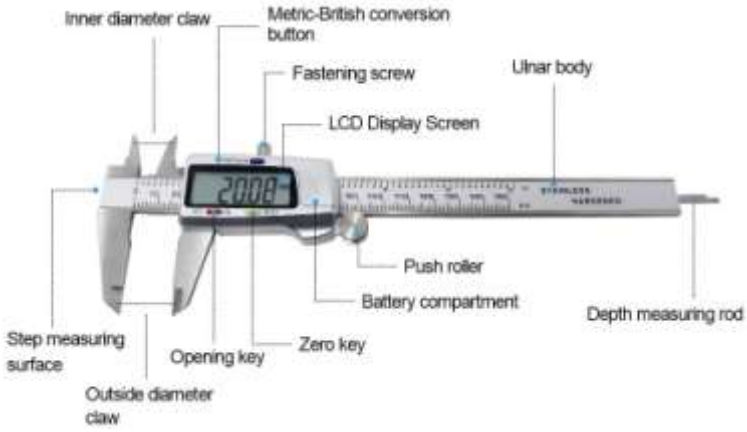

Figure 3: Digital Vernier - VINCA DCLA-0605

II.III Digital close range photogrammetry (CRP)

Photogrammetry is a surveying method that uses (as the name suggests) camerasto take images of a target object and retrieve different geometrical information of that object. When the target object is photographed, information of that object and its surroundings are stored in images, hence every captured point can be extracted back by using mathematical models that mainly depends on understanding the way light rays reflect from the target object reaching the lens of the camera to finally settle in specific directions and manner in a sensor (surface) inside the camera. This way, real points captured by the camera are converted from 3D entities to 2D entities which means there exist some loss of information. Hence, there exist two scientific terms that should be well understood in order to better describe the geometries of the camera, which are: interior orientation & exterior orientation. In brief words, interior orientation is a set of parameters that when well obtained, the projection process happening inside the camera could be described accurately. These parameters are: the Principal Point, the Principal Distance and the Parameters of functions describing imaging errors. Exterior orientation on the other hand, simply describe the location and orientation of the camera itself with respect to the global system of the target object [6].

There exist two types of photogrammetric cameras: Metric and Non-Metric. The use of each type will heavily affect the type of the mathematical model being used to transform the collected 3D points from image space to the global space, as follows:

(a) Metric Camera: These are cameras with known and stable initial interior orientation parameters.[6]
(b) Non-Metric Camera: These are cameras that don't have a photogrammetric reference system which means that interior orientation parameters are unknowns in this case.

The use of metric cameras means that we will have to calibrate the initial interior orientation parameters to use them in the transformation mathematical model. On the other hand,the use of non-metric cameras (as our case in this study) will evade this problem by solving the set of collinearity equations using Direct Linear Transformation method (DLT) proposed by (Abdel-Aziz and Karara 1971), which is the case in this study [28].

II.IV Terrestrial Laser Scanning (TLS)

Laser scanners are instruments that uses laser light as a mean to measure distance towards a target object. These devices works automatically and have the ability to capture huge amount of 3D coordinates for a target object in a very short time that reaches 1 million points per second [25]. In addition to the coordinates of every scanned point, laser scanners alsocollect information about the intensity of the reflected laser light which is useful to obtain and record an image of the scanned object [6].Laser scanners are very useful in collecting huge amount of points which is called "point cloud". These point clouds can be used by sophisticated software programs to obtain other useful data formats like 3D mesh, solid surfaces, etc. By using these data, very complicated and difficult engineering tasks can become handy when performed by a special software like BIM, CAD, others. Laser scanners are available in many shapes (static, mobile on vehicles, mobile on air drones, hand held, etc.) and vary in their sight range. There exist some models that can do scanning for distances up to 100 m and others up to 300 m. They also vary in their scanning speed from 100,000 points/sec up to 1,000,000 points/sec.

III. Experimentdescription

The experiment performed under this research aims to investigate and compare the methodologies mentioned in this study in monitoring and detecting cracks and deflection in a loaded reinforced concrete beam. The beam was loaded in a 4-point load test as shown in the following figures. The test lab is composed of a steel frame, two movable I-beam girders functioning as a support for test beams,a double acting hydraulic cylinder (to apply the desired load)of 150-ton capacity and 150 mm maximum stroke connected to a hydraulic pump, a load cell of 225-ton capacity to measure the applied load.

Figure 4: Test beam – No Loading case

Figure 5: Test beam under loading

The reinforced concrete test beam has dimensions of 1100 mm length ×200 mm depth × 100 mm width. Steel reinforcement details were 3 ϕ 12 mm (lower bars), 2 ϕ 10 mm (upper bars), with 4 ϕ8 mm (see figure below).

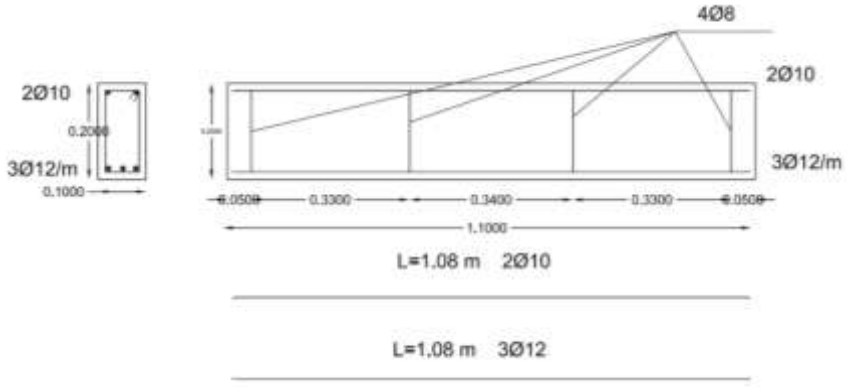

Figure 6: Reinforcement of test beam

The materials of the reinforced concrete beam:

- Cement: Portland cement CEM I N 52.5. Its chemical and physical characteristics comply with the Egyptian Standard Specification (E.S.S. 4756-1/2009).
- Fine aggregate: Clean natural sand of specific gravity 2.71 t/m^3.
- Coarse aggregate: Crushed dolomite of specific gravity 2.65 t/m^{3}and water absorption value of 0.6%.
- Steel Reinforcement: Mild steel (Grade st.37) used in main mesh and rounded plain bars of diameter 8 mm.

To measure the beam deflection, a LVDT (of capacity 150 mm) is placed under the test beam at the mid span of its length. The readings of both the LVDT and the load cell were monitored by a data logger connected to both devices that shows a continuous record of each reading (defection value & applied load).

Three loading cases have been applied to the test beam, which are: Ultimate case, Crack case & Failure case. For the photogrammetric system to function properly, 22 code targets were attached to the side surface of the test beam as shown in the previous figures. These targets were observed by the different methods under considerations of this study (Total station, Photogrammetry& Laser scanner) and the results were collected for each of them.

Figure 7:View of the experiment

IV. Equipment

IV.I Linear Variable Differential Transformer (LVDT) sensor(LD320-25)

The technical specifications of the LVDT (LD320-25) sensor is as follows:

- up to 75 mm travel
- <0.2% Linearity
- Rugged 19 mm Dia. Stainless Steel Body
- Rigid Stainless Steel Carrier
- IP67 Protection
- Guided Core for Easy Installation

Figure 8: LVDT – LD320-25

IV.II VINCA DCLA-0605 Electronic Digital Vernier

The technical specifications of the VINCA DCLA-0605 Electronic Digital Vernier is as follows:

- Material is stainless steel.
- Total lengthis 6-in/150-mm.
- Accuracy of 0.001 in (0.02mm)
- Resolution of 0.0005 in (0.01 mm).

Figure 9: Digital Vernier - VINCA DCLA-0605

IV.III Total station SOKKIA CX105

A total station SOKKIA CX-105 shown in the following figure was used in this study. The technical specifications of the total station is listed in Table1 [29] [30].

Figure 10: SOKKIA CX105 total station

Table 1: Technical specification of SOKKIA CX-105

Resolution of display	1/5 in. 0.005/0.02 mil
Accuracy	5 in.
Laser beam (mode ofReflector-less)	Class 3R/Prism/sheet mode: Class 1
Range of reflector-less mode	Up to 0.5 km
Range of prism mode	1.3–4000 m/Under good conditions: to5000 m
Resolution Display	Fine/Rapid: 0.001 m/0.01 ft./1/8 in
Tracking	0.01 m/0.1 ft./1/2 in
Accuracy Reflector-less	(3+2 ppm x D) mm
Prism Mode	(2+2 ppm x D) mm
Zooming in	30 x
Data Storage	10,000 points Internal storage
Communications	USB memory
Temperature ofOperating	-20 to + 50 C
Operating Time	Approx. 36 h

IV.IV Digital cameras

A Nikon D7200 camera was used for photogrammetry in this study. The technical specificationsof the camera is as follows [31].

- 24.2 MP CMOS sensor
- 2016 pixel RGB metering sensor
- 1/8000 sec maximum shutter speed
- 3.2", 1.2M dot RGBW LCD display
- Dual SD card slots
- Wi-Fi with NFC

Figure 11: Nikon D7200 Photogrammetric Camera

IV.V Terrestrial laser scanner TOPCON GLS-2000

A medium range laser scanner, TOPCON model GLS-2000, was used in this study. The technical specifications of the camera is listed in table 2. [32]

Figure 12: TOPCON GLS-2000 – Laser Scanner

Table 2: Technical specification of the Topcon GLS-2000

Performance of the system	
(Standard, High speed, Low power) mode	(350, 210, 210) m at 90%
Accuracy of the points	
Distance	3.5 mm (1 - 150 m)
Angle	6 second
Type	Liquid 2-axis tilt sensor
Compensation range	± 6 min.
Target detection accuracy	3 seconds at 50 m
Laser scanning system	
Type	Pulse (time of flight); precise scan tech II
Laser class	3R (high speed / standard), 1M (low power)
Scan rate (high speed)	Up to 120,000 pts/sec
Spot size	4 mm at 20 m (FWHM)
Field of view (per scan)	360^0 (H) / 270^0 (V)
Color digital imaging	
Wide angle	170^0 Diagonal
Telephoto	11.90 (H) / 8.90 (V)

V. Data collection and Results:

As stated before, the deflection of the test beam was measured by the LVDT located at the middle of the concrete beam using, at each of the three loading cases (ultimate, crack, and failure). The total station SOKKIA CX105 was also used to observe and monitor the 22 coded control sites and the crack width was measured using the digital Vernier. This is shown in figures (13& 14). The following is a table with the results:

Figure 13: View of Photo-modeler (Software used for Photogrammetry)

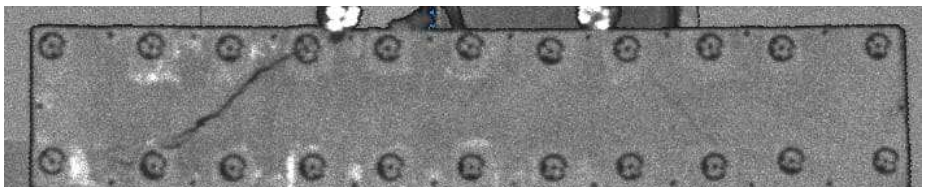

Figure 14:View of the test beam observed from TLS

Table 3: Resultsof No Loading case

Load = 0 KN							
LVDT	Deflection at Centre	Δ (mm) = 0					
Vernier	width of crack (mm)	width 1		width 2		width 3	
	crack 1	0		0		0	
	crack 2	0		0		0	
Total station	point no	coordinates (m)					
		X		Y		Z	
	1	94.386		93.884		1.051	
	2	94.512		93.884		1.052	
	3	94.612		93.885		1.053	
	4	94.711		93.885		1.052	
	5	94.811		93.885		1.052	
	6	94.912		93.885		1.052	
	7	95.012		93.884		1.051	
	8	95.112		93.884		1.052	
	9	95.211		93.885		1.052	
	10	95.313		93.885		1.051	
	11	95.437		93.884		1.051	
	12	95.435		93.886		1.203	
	13	95.310		93.884		1.202	
	14	95.211		93.885		1.201	
	15	95.113		93.885		1.201	
	16	95.013		93.885		1.202	
	17	94.912		93.886		1.202	
	18	94.812		93.884		1.201	
	19	94.711		93.885		1.201	
	20	94.614		93.885		1.202	
	21	94.513		93.884		1.202	
	22	94.391		93.884		1.201	
Photogrammetry point Deflection	point no	coordinates (mm)			standard deviation (mm)		
		X	Y	Z	δx	δy	δz
	1	1337.018	-25.6643	61.7372	0.115056	0.204881	0.102016
	2	1460.326	-24.8859	62.82944	0.135	0.206	0.097

	3	1560.388	-27.1936	62.07043	0.115	0.193	0.095
	4	1662.083	-24.6464	61.73823	0.114	0.196	0.094
	5	1760.211	-27.0767	61.98158	0.12	0.206	0.094
	6	1860.741	-27.6218	61.15542	0.126	0.216	0.094
	7	1959.29	-26.2782	62.89833	0.119	0.215	0.09
	8	2059.762	-26.6142	64.10873	0.119	0.216	0.09
	9	2159.704	-26.3126	62.95336	0.117	0.212	0.089
	10	2259.62	-27.2963	61.77417	0.112	0.206	0.09
	11	2385.685	-25.8921	62.25777	0.101	0.195	0.088
	12	2384.993	-26.763	211.8741	0.102	0.187	0.093
	13	2261.428	-26.7167	212.9951	0.114	0.192	0.092
	14	2161.101	-25.0365	212.7223	0.12	0.195	0.087
	15	2060.61	-27.0225	213.933	0.124	0.196	0.086
	16	1961.345	-26.616	213.8707	0.126	0.196	0.086
	17	1859.394	-26.8368	211.7885	0.123	0.193	0.086
	18	1761.117	-27.2163	212.03	0.12	0.196	0.091
	19	1659.856	-25.5346	212.7774	0.113	0.195	0.091
	20	1561.894	-24.6276	213.5556	0.11	0.201	0.088
	21	1460.453	-26.2808	211.6486	0.137	0.233	0.089
	22	1335.451	-25.9925	213.2441	0.208	0.294	0.088
Load = 0 KN(Continue)							
Photogrammetry cracks	width of crack (mm)	width 1		width 2		width 3	
	crack 1	0		0		0	
	crack 2	0		0		0	
Laser scanner point Deflection	point no	coordinates (mm)			standard deviation (mm)		
		X	Y	Z	δx	δy	δz
	1	1335.061	-27.366	63.410	0.121493	0.205902	0.104678
	2	1460.260	-24.791	62.729	0.136539	0.207612	0.100569
	3	1560.850	-26.300	61.609	0.118229	0.195254	0.101201
	4	1660.322	-25.096	64.084	0.123297	0.196526	0.10061
	5	1759.954	-24.870	63.343	0.122285	0.211203	0.095017
	6	1859.935	-26.432	62.709	0.126259	0.216343	0.10018
	7	1960.918	-25.370	62.277	0.121297	0.216894	0.092374
	8	2060.692	-25.361	62.620	0.119954	0.216864	0.096336
	9	2161.131	-26.425	62.230	0.117051	0.220192	0.097092
	10	2261.056	-27.460	62.095	0.116913	0.210478	0.097734
	11	2386.194	-24.716	61.665	0.109608	0.199183	0.095096
	12	2385.135	-26.551	214.101	0.106575	0.187125	0.095759
	13	2259.412	-26.823	213.476	0.121534	0.194898	0.099724
	14	2159.874	-25.124	211.269	0.122908	0.197873	0.095746
	15	2059.747	-24.765	211.902	0.128546	0.198671	0.093947
	16	1959.297	-25.580	212.989	0.134728	0.197125	0.093136
	17	1859.844	-27.601	212.134	0.129179	0.201841	0.087358
	18	1760.005	-26.445	213.077	0.124663	0.196872	0.100079
	19	1661.841	-25.279	211.800	0.116616	0.203661	0.091107
	20	1561.090	-26.575	212.364	0.112909	0.206395	0.096645
	21	1461.039	-25.251	211.448	0.140062	0.233134	0.090454
	22	1335.764	-25.914	213.758	0.211908	0.2979	0.096605
Laser scanner cracks	width of crack (mm)	width 1		width 2		width 3	
	crack 1	0		0		0	
	crack 2	0		0		0	

Table 4:Results of Ultimate case, 44 KN load

Load = 44 KN				
LVDT	Deflection at Centre	Δ (mm) = 1.18 mm		
Vernier	width of crack (mm)	width 1	width 2	width 3
	crack 1	0.402	0.662	0.381
	crack 2	0.915	1.581	0.676
Total station	point no	coordinates (m)		
		X	Y	Z
	1	94.384	93.884	1.052
	2	94.511	93.884	1.052
	3	94.612	93.885	1.053
	4	94.711	93.885	1.052
	5	94.811	93.885	1.051
	6	94.912	93.885	1.051
	7	95.012	93.885	1.050
	8	95.112	93.885	1.052

	9	95.211		93.886		1.052	
	10	95.314		93.886		1.051	
	11	95.439		93.884		1.052	
	12	95.437		93.885		1.203	
	13	95.311		93.885		1.202	
	14	95.211		93.884		1.201	
	15	95.113		93.886		1.201	
	16	95.013		93.884		1.201	
	17	94.912		93.885		1.201	
	18	94.812		93.886		1.200	
	19	94.711		93.885		1.201	
	20	94.614		93.885		1.202	
	21	94.512		93.885		1.202	
	22	94.389		93.885		1.202	
Photogrammetry point Deflection	point no	coordinates (mm)			standard deviation (mm)		
		X	Y	Z	δx	δy	δz
	1	1334.976	-25.432	62.754	0.158	0.210	0.082
	2	1459.322	-25.425	62.739	0.106	0.182	0.079
	3	1560.338	-27.063	61.974	0.092	0.181	0.078
	4	1661.952	-25.403	61.657	0.091	0.187	0.078
	5	1760.174	-26.442	60.801	0.097	0.196	0.078
	6	1860.905	-27.829	60.379	0.102	0.202	0.078
	7	1959.329	-25.940	61.840	0.105	0.205	0.078
	8	2059.902	-25.926	64.000	0.104	0.204	0.078
	9	2159.760	-25.958	62.933	0.099	0.200	0.078
	10	2260.772	-26.358	61.670	0.092	0.193	0.076
	11	2387.859	-25.963	62.955	0.086	0.185	0.075
	12	2387.177	-27.801	212.320	0.087	0.179	0.075
	13	2262.557	-25.989	213.106	0.097	0.179	0.075
	14	2161.185	-26.017	212.623	0.105	0.183	0.074
	15	2060.740	-26.428	213.820	0.110	0.186	0.074
	16	1961.476	-27.613	212.832	0.111	0.187	0.074
	17	1859.446	-27.406	210.675	0.108	0.186	0.074
	18	1761.259	-25.786	210.996	0.100	0.183	0.073
	19	1659.962	-25.354	212.701	0.093	0.261	0.082
	20	1562.050	-24.831	213.366	0.090	0.185	0.073
	21	1459.284	-25.601	211.658	0.107	0.206	0.081
	22	1333.323	-24.914	213.915	0.154	0.245	0.077
Load = 44 KN (Continue)							
Photogrammetry cracks	width of crack (mm)	width 1		width 2		width 3	
	crack 1	0.462		0.745		0.434	
	crack 2	1.001		1.756		0.762	
Laser scanner point Deflection	point no	coordinates (mm)			standard deviation (mm)		
		X	Y	Z	δx	δy	δz
	1	1333.004	-27.432	64.493	0.160	0.219	0.091
	2	1458.975	-25.285	62.399	0.108	0.183	0.082
	3	1560.624	-26.286	61.221	0.097	0.189	0.080
	4	1660.076	-25.969	63.755	0.091	0.191	0.080
	5	1759.690	-24.378	62.033	0.099	0.197	0.085
	6	1860.020	-26.906	62.092	0.106	0.205	0.085
	7	1961.118	-25.153	60.970	0.110	0.212	0.081
	8	2061.008	-24.795	62.499	0.105	0.210	0.081
	9	2161.495	-26.056	62.008	0.101	0.202	0.086
	10	2262.212	-26.736	61.911	0.093	0.199	0.082
	11	2388.264	-24.961	62.293	0.090	0.187	0.085
	12	2387.443	-27.663	214.571	0.087	0.182	0.076
	13	2260.448	-26.225	213.410	0.100	0.182	0.075
	14	2159.896	-26.027	210.924	0.106	0.190	0.083
	15	2059.975	-24.365	211.522	0.111	0.186	0.074
	16	1959.515	-26.469	211.803	0.116	0.192	0.075
	17	1860.005	-28.378	210.882	0.113	0.190	0.080
	18	1760.033	-25.174	211.940	0.109	0.183	0.081
	19	1662.081	-25.045	211.415	0.094	0.262	0.087
	20	1561.282	-26.927	212.184	0.099	0.185	0.081
	21	1459.642	-24.602	211.741	0.117	0.209	0.087
	22	1333.523	-24.796	214.611	0.157	0.251	0.079
Laser scanner cracks	width of crack (mm)	width 1		width 2		width 3	
	crack 1	----		----		----	

	crack 2	1.156	1.834	----

Table 5: Results of Crack case, 115.6 KN load

Load = 115.6 KN							
LVDT	Deflection at Centre	Δ (mm) = 3.08 mm					
Vernier	width of crack (mm)	width 1		width 2		width 3	
	crack 1	0.481		1.121		0.769	
	crack 2	1.052		2.371		1.602	
Total station	point no	coordinates (m)					
		X		Y		Z	
	1	94.383		93.885		1.053	
	2	94.511		93.885		1.051	
	3	94.612		93.885		1.052	
	4	94.711		93.884		1.050	
	5	94.811		93.886		1.049	
	6	94.912		93.885		1.050	
	7	95.012		93.885		1.048	
	8	95.112		93.886		1.050	
	9	95.211		93.886		1.051	
	10	95.314		93.886		1.050	
	11	95.440		93.884		1.053	
	12	95.438		93.884		1.204	
	13	95.312		93.886		1.200	
	14	95.211		93.883		1.200	
	15	95.113		93.886		1.200	
	16	95.013		93.884		1.199	
	17	94.912		93.885		1.199	
	18	94.812		93.887		1.198	
	19	94.711		93.885		1.199	
	20	94.614		93.885		1.200	
	21	94.511		93.886		1.202	
	22	94.388		93.886		1.203	
Photogrammetry point Deflection	point no	coordinates (mm)			standard deviation (mm)		
		X	Y	Z	δx	δy	δz
	1	1334.292	-25.290	64.168	0.160	0.219	0.091
	2	1459.302	-24.226	61.333	0.108	0.183	0.082
	3	1560.285	-26.777	60.992	0.097	0.189	0.080
	4	1661.612	-26.015	59.493	0.091	0.191	0.080
	5	1760.090	-25.929	58.621	0.099	0.197	0.085
	6	1860.750	-28.343	58.952	0.106	0.205	0.085
	7	1959.578	-25.562	59.821	0.110	0.212	0.081
	8	2059.820	-25.831	61.874	0.105	0.210	0.081
	9	2159.879	-25.489	61.925	0.101	0.202	0.086
	10	2260.818	-25.559	60.453	0.093	0.199	0.082
	11	2388.978	-26.070	64.021	0.090	0.187	0.085
	12	2388.156	-29.024	213.263	0.087	0.182	0.076
	13	2263.517	-25.404	210.954	0.100	0.182	0.075
	14	2161.291	-26.541	211.116	0.106	0.190	0.083
	15	2060.817	-25.721	212.517	0.111	0.186	0.074
	16	1961.421	-28.586	210.483	0.116	0.192	0.075
	17	1859.714	-28.044	208.619	0.113	0.190	0.080
	18	1761.435	-24.374	209.018	0.109	0.183	0.081
	19	1660.278	-24.976	210.513	0.094	0.262	0.087
	20	1562.361	-25.089	211.284	0.099	0.185	0.081
	21	1458.038	-24.977	211.804	0.117	0.209	0.087
	22	1332.324	-24.321	214.971	0.157	0.251	0.079
Load = 115.6 KN (Continue)							
Photogrammetry cracks	width of crack (mm)	width 1		width 2		width 3	
	crack 1	0.554		1.261		0.821	
	crack 2	1.154		2.649		1.802	
Laser scanner point Deflection	point no	coordinates (mm)			standard deviation (mm)		
		X	Y	Z	δx	δy	δz
	1	1332.455	-27.140	65.606	0.166	0.226	0.098
	2	1458.755	-24.638	61.214	0.115	0.190	0.087
	3	1560.593	-26.426	60.214	0.102	0.197	0.084
	4	1659.657	-26.466	61.553	0.100	0.196	0.087

	5	1759.567	-23.842	59.860	0.108	0.199	0.087
	6	1860.022	-27.291	60.913	0.107	0.213	0.094
	7	1961.222	-24.736	59.214	0.111	0.214	0.090
	8	2061.262	-24.354	60.159	0.114	0.217	0.089
	9	2161.668	-25.742	61.100	0.108	0.210	0.090
	10	2262.282	-26.385	60.724	0.100	0.205	0.084
	11	2389.481	-24.937	64.102	0.099	0.194	0.085
	12	2388.786	-28.588	215.945	0.092	0.183	0.081
	13	2261.416	-25.664	211.382	0.110	0.189	0.082
	14	2159.893	-27.193	209.411	0.114	0.193	0.089
	15	2059.977	-23.632	210.018	0.120	0.194	0.080
	16	1959.490	-27.651	209.623	0.116	0.195	0.084
	17	1860.375	-29.065	208.658	0.119	0.199	0.081
	18	1760.081	-23.570	209.498	0.118	0.184	0.087
	19	1662.036	-25.041	208.956	0.096	0.264	0.091
	20	1561.180	-27.139	210.182	0.100	0.186	0.082
	21	1458.538	-23.750	212.132	0.120	0.209	0.088
	22	1332.204	-24.459	215.297	0.164	0.260	0.082
Laser scanner cracks	width of crack (mm)	width 1		width 2		width 3	
	crack 1	----		1.362		----	
	crack 2	1.202		2.943		1.886	

Table 6:Results of Failure case, at 153.1 KN load

Load = 153.1 KN							
LVDT	Deflection at Centre	Δ (mm) = 4.26 mm					
Vernier	width of crack (mm)	width 1		width 2		width 3	
	crack 1	0.603		1.512		0.871	
	crack 2	1.281		2.981		1.951	
Total station	point no	coordinates (m)					
		X		Y		Z	
	1	94.381		93.885		1.054	
	2	94.509		93.886		1.050	
	3	94.612		93.885		1.050	
	4	94.711		93.884		1.048	
	5	94.811		93.886		1.048	
	6	94.912		93.884		1.048	
	7	95.012		93.885		1.047	
	8	95.112		93.886		1.048	
	9	95.211		93.886		1.049	
	10	95.315		93.887		1.050	
	11	95.442		93.884		1.053	
	12	95.440		93.883		1.205	
	13	95.313		93.886		1.201	
	14	95.211		93.883		1.199	
	15	95.113		93.887		1.198	
	16	95.013		93.883		1.197	
	17	94.912		93.885		1.196	
	18	94.812		93.888		1.196	
	19	94.711		93.886		1.197	
	20	94.614		93.885		1.198	
	21	94.511		93.884		1.199	
	22	94.386		93.887		1.203	
Photogrammetry point Deflection	point no	coordinates (mm)			standard deviation (mm)		
		X	Y	Z	δx	δy	δz
	1	1332.317	-25.5585	64.75376	0.164	0.209	0.091
	2	1456.506	-24.6797	60.88614	0.113	0.187	0.088
	3	1559.833	-27.4307	58.51425	0.104	0.211	0.092
	4	1661.62	-25.9273	57.30553	0.099	0.188	0.089
	5	1759.771	-26.5241	57.50849	0.104	0.192	0.089
	6	1861.486	-27.9359	56.51323	0.11	0.194	0.09
	7	1959.699	-25.9069	57.98641	0.113	0.194	0.09
	8	2059.836	-26.0504	60.04528	0.111	0.192	0.09
	9	2160.392	-25.6114	59.53903	0.106	0.188	0.09
	10	2261.931	-25.9954	60.11236	0.098	0.182	0.089
	11	2391.649	-26.3314	64.90998	0.093	0.175	0.087
	12	2390.803	-29.3619	215.3805	0.094	0.167	0.086
	13	2264.925	-25.4896	211.9616	0.104	0.17	0.086
	14	2161.46	-26.5854	209.3363	0.113	0.174	0.086

	15	2061.095	-26.4844	210.4611	0.12	0.178	0.085
	16	1961.673	-28.6456	208.7922	0.121	0.181	0.085
	17	1859.811	-28.5702	205.1957	0.117	0.182	0.084
	18	1761.806	-24.8416	206.2081	0.108	0.182	0.084
	19	1660.806	-25.1254	208.4571	0.1	0.182	0.083
	20	1561.926	-25.3965	208.6375	0.096	0.184	0.082
	21	1457.802	-25.5511	208.9534	0.11	0.191	0.081
	22	1329.485	-24.5436	215.3577	0.156	0.214	0.079

Load = 153.1 KN (Continue)							
Photogrammetry cracks	width of crack (mm)	width 1		width 2		width 3	
	crack 1	0.695		1.711		0.992	
	crack 2	1.302		2.888		1.975	
Laser scanner point Deflection	point no	coordinates (mm)			standard deviation (mm)		
		X	Y	Z	δx	δy	δz
	1	1330.064	-27.975	66.429	0.170	0.218	0.099
	2	1456.352	-24.074	60.081	0.114	0.193	0.097
	3	1560.326	-26.481	57.927	0.106	0.214	0.097
	4	1659.534	-26.315	59.924	0.108	0.193	0.091
	5	1758.916	-24.785	58.796	0.111	0.195	0.092
	6	1860.863	-26.727	57.746	0.112	0.201	0.094
	7	1961.534	-24.813	58.094	0.121	0.204	0.095
	8	2061.104	-24.327	57.821	0.120	0.200	0.095
	9	2161.530	-26.342	58.929	0.110	0.197	0.096
	10	2263.362	-26.503	60.891	0.103	0.190	0.091
	11	2391.505	-25.725	63.774	0.094	0.182	0.094
	12	2390.856	-29.394	217.436	0.096	0.170	0.090
	13	2262.536	-25.882	212.528	0.105	0.171	0.087
	14	2160.912	-27.741	208.436	0.118	0.176	0.093
	15	2059.810	-23.868	207.599	0.126	0.179	0.089
	16	1960.027	-27.110	207.730	0.127	0.188	0.087
	17	1860.837	-29.169	204.908	0.124	0.192	0.088
	18	1760.345	-23.826	207.130	0.110	0.185	0.088
	19	1662.004	-25.074	206.496	0.103	0.184	0.089
	20	1561.972	-26.954	207.781	0.097	0.191	0.087
	21	1458.801	-23.770	209.270	0.120	0.195	0.089
	22	1330.084	-24.065	216.642	0.159	0.222	0.082
Laser scanner cracks	width of crack (mm)	width 1		width 2		width 3	
	crack 1	00		1.915		1.067	
	crack 2	1.351		2.998		1.897	

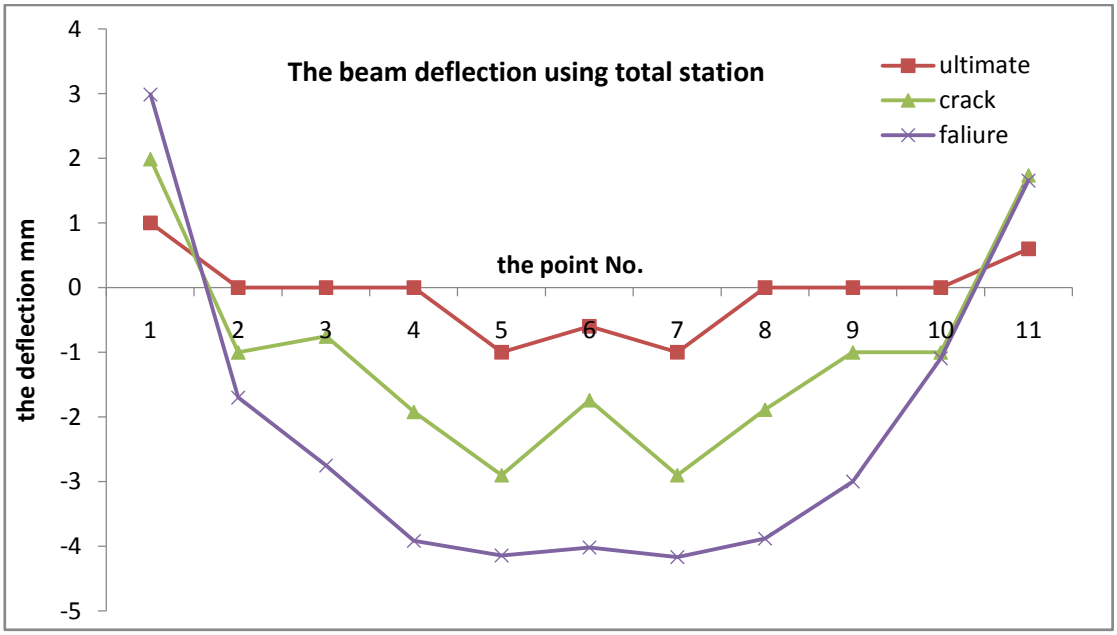

Figure 15: The beam deflection using total station in 3 cases (ultimate, crack, failure)

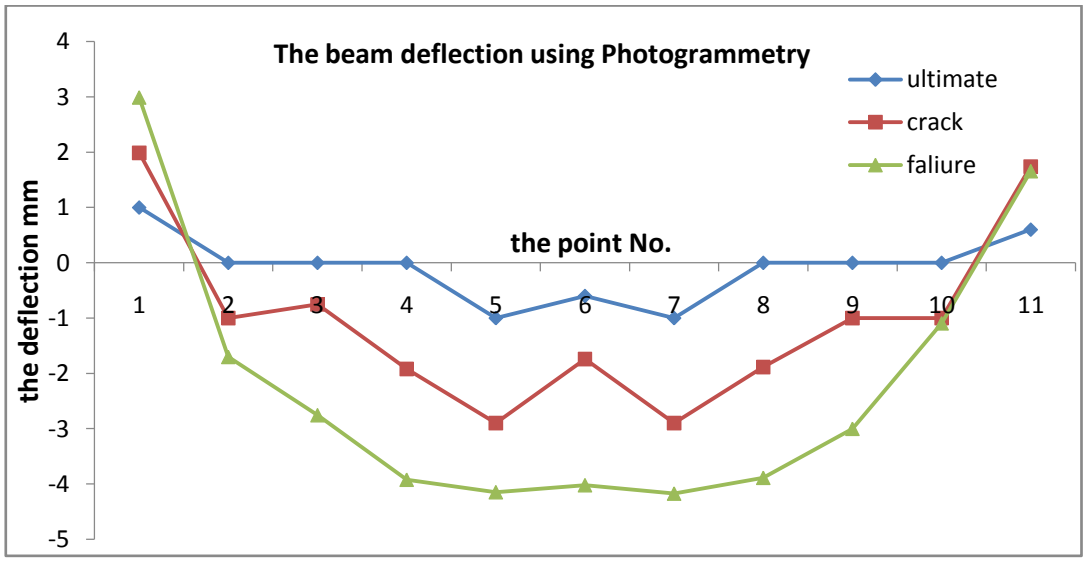

Figure 16: The beam deflection using Photogrammetry in 3 cases (ultimate, crack, failure)

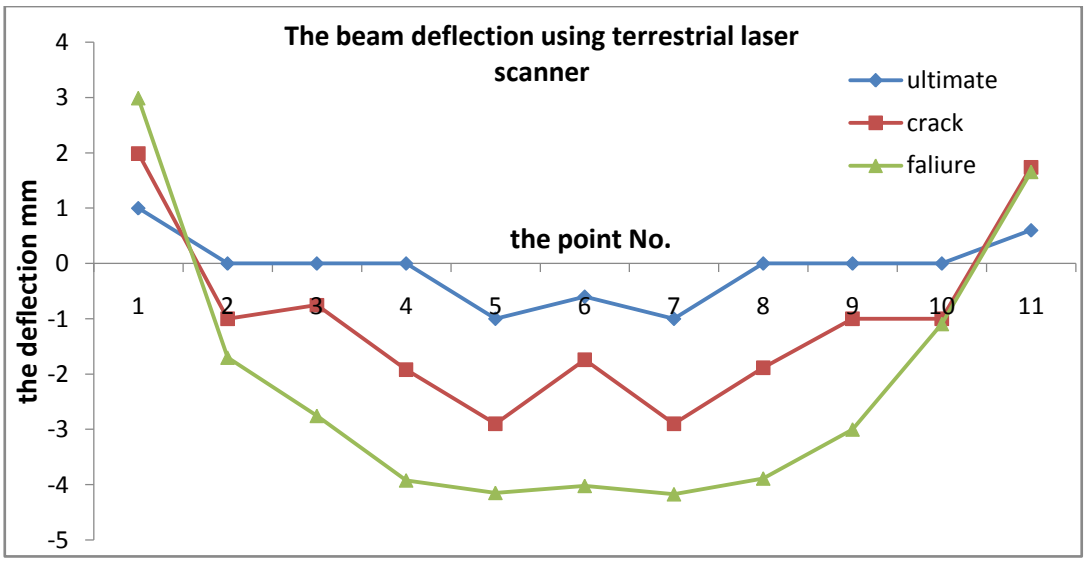

Figure 17: The beam deflection using Laser scanner in 3 cases (ultimate, crack, failure)

VI. Conclusion

Three Surveying techniques have been used in this study (Photogrammetry, Laser scanner & Total station) and the results obtained in the experiment (depending on the experiment environment and the accuracy of the used instruments) showed that all the three techniques are possible for use in detecting reinforced concretecracks and deformations. After comparing their results to traditional methods (LVDT & Vernier), it is found that:

1) For beam deflection: The Root Mean Square Error (RMSE) was calculated for each technique in reference to LVDT readings. RMSE of total station results is 0.28, RMSE of photogrammetry is 0.46 and RMSE of laser scanner is 0.47. Thatmeans total station has provided the closest results to LVDT then follows photogrammetry then finally Laser scanner.

2) For crack width:RMSE values was calculated for photogrammetry and laser scanner results technique in reference to Vernier readings. RMSE of photogrammetry is 0.1 and RMSE of laser scanner is 0.2. That means photogrammetry provided the closest results to Vernier readings compared to Laser scanner.

References

[1]. Pan, Hongke, and Ling Pi. "Study on cracks in concrete structures and the database." IOP Conference Series: Earth and Environmental Science. Vol. 189. No. 2. IOP Publishing, 2018.
[2]. Kwak, Hyo-Gyoung, Soo-Jun Ha, and Jin-Keun Kim. "Non-structural cracking in RC walls: Part I. Finite element formulation." Cement and Concrete Research 36.4 (2006): 749-760.
[3]. Yang, Shangtong. Concrete crack width under combined reinforcement corrosion and applied load. Diss. University of Greenwich, 2010.
[4]. Control of Cracking in Concrete: State of the ArtTransportation Research BoardBasic Research and Emerging Technologies Related to Concrete Committee, October 2006Transportation Research Board500 Fifth Street, NW, Washington, DC 20001, www.TRB.org
[5]. Detchev, I., et al. "DEFORMATION MONITORING WITH OFF-THE-SHELF DIGITAL CAMERAS FOR CIVIL ENGINEERING FATIGUE TESTING." International Archives of the Photogrammetry, Remote Sensing & Spatial Information Sciences 45 (2014).
[6]. Luhmann, Thomas, et al. Close range photogrammetry: principles, techniques and applications. Vol. 3. Dunbeath: Whittles publishing, 2006.
[7]. Galantucci, Rosella Alessia, and Fabio Fatiguso. "Advanced damage detection techniques in historical buildings using digital photogrammetry and 3D surface analysis." Journal of Cultural Heritage 36 (2019): 51-62.
[8]. Jiang, Ruinian, David V. Jáuregui, and Kenneth R. White. "Close-range photogrammetry applications in bridge measurement: Literature review." Measurement 41.8 (2008): 823-834.
[9]. Riveiro, Belén, et al. "Validation of terrestrial laser scanning and photogrammetry techniques for the measurement of vertical underclearance and beam geometry in structural inspection of bridges." Measurement 46.1 (2013): 784-794.
[10]. Riveiro, B., et al. "Photogrammetric 3D modelling and mechanical analysis of masonry arches: An approach based on a discontinuous model of voussoirs." Automation in Construction 20.4 (2011): 380-388.
[11]. Jiang, Ruinian, and David V. Jauregui. "Development of a digital close-range photogrammetric bridge deflection measurement system." Measurement 43.10 (2010): 1431-1438.
[12]. Solla, M., et al. "Non-destructive methodologies in the assessment of the masonry arch bridge of Traba, Spain." Engineering Failure Analysis 18.3 (2011): 828-835.
[13]. Stull, C. J., and C. J. Earls. "A rapid assessment methodology for bridges damaged by truck strikes." Steel Compos. Struct 9.3 (2009): 223-237.
[14]. Teza, Giordano, Antonio Galgaro, and Francesca Moro. "Contactless recognition of concrete surface damage from laser scanning and curvature computation." Ndt & E International 42.4 (2009): 240-249.
[15]. Pucinotti, Raffaele, and Milena Tripodo. "The Fiumarella bridge: Concrete characterisation and deterioration assessment by nondestructive testing." International Journal of Microstructure and Materials Properties 4.1 (2009): 128.
[16]. Lubowiecka, Izabela, et al. "Historic bridge modelling using laser scanning, ground penetrating radar and finite element methods in
[17]. Poptean, S. I., et al. "Applications of Terrestrial Laser Scanning for deformation analyses of an adaptive supporting structure."
[18]. Zaczek-Peplinska, Janina, and Maria Elżbieta Kowalska. "Terrestrial laser scanning in monitoring hydrotechnical objects." Journal of Ecological Engineering 17.4 (2016).
[19]. Arias, Pedro, et al. "3D modeling and section properties of ancient irregular timber structures by means of digital photogrammetry." Computer-Aided Civil and Infrastructure Engineering 22.8 (2007): 597-611.
[20]. Ordóñez, Celestino, et al. "Measuring building façades with a low-cost close-range photogrammetry system." Automation in Construction 19.6 (2010): 742-749.
[21]. Alshawabkeh, Yahya, Norbert Haala, and Dieter Fritsch. "A new true ortho-photo methodology for complex archaeological application." Archaeometry 52.3 (2010): 517-530.
[22]. Arias, P., et al. "ORTHOIMAGE-BASED DOCUMENTATION OF ARCHAEOLOGICAL STRUCTURES: THE CASE OF A MEDIAEVAL WALL IN PONTEVEDRA, SPAIN." Archaeometry 53.4 (2011): 858-872.
[23]. Luhmann, Thomas. "Close range photogrammetry for industrial applications." ISPRS journal of photogrammetry and remote sensing 65.6 (2010): 558-569.
[24]. Porteiro, Jacobo, et al. "A refrigerated web camera for photogrammetric video measurement inside biomass boilers and combustion analysis." Sensors 11.2 (2011): 1246-1260.
[25]. Abdel, Mostafa. "3d laser scanners: history, applications, and future." Assiut University. October (2011).
[26]. Historic England. "3D Laser Scanning for Heritage: Advice and Guidance on the Use of Laser Scanning in Archaeology and Architecture." (2018).
[27]. Mukupa, Wallace, et al. "A review of the use of terrestrial laser scanning application for change detection and deformation monitoring of structures." Survey review 49.353 (2017): 99-116.
[28]. Abdel-Aziz, Yousset I., Hauck Michael Karara, and Michael Hauck. "Direct linear transformation from comparator coordinates into object space coordinates in close-range photogrammetry." Photogrammetric engineering & remote sensing 81.2 (2015): 103-107.
[29]. Fawzy, Hossam El-Din. "The impact of vibration on the accuracy of digital surveying instruments." Civil Engineering Journal 5.3 (2019): 515-527.
[30]. SOKKIA, SOKKIA CX-105, https://www.vpcivil.co.in/sokkiacx-105-total-station-india/ (published 2019).
[31]. Nikon, Nikon D7200, https://www.nikonusa.com/en/nikonproducts/product/dslr-cameras/d7200.html (published 2019).
[32]. TOPCON, TOPCON GLS-2000, https://www.topconpositioning.com/mass-data-and-volume-collection/laser-scanners/gls-2000 (published 2019).

Magda Farhan. "3D Laser Scanningand Close-Range Photogrammetryfor Observation and Measuring the Reinforced Concrete (RC) StructuralCracks& Deflection". *IOSR Journal of Mechanical and Civil Engineering (IOSR-JMCE)*, 19(4), 2022, pp. 08-23.